Mon. Not. R. Astron. Soc. **366,** 1520–1528 (2006) doi:10.1111/j.1365-2966.2005.09931.x

The evolutionary status of the white dwarf companion of the binary pulsar PSR J1713+0747

O. G. Benvenuto,[1,2⋆†] R. D. Rohrmann[3⋆‡] and M. A. De Vito[2⋆§]

[1]*Departamento de Astronomía y Astrofísica, Pontificia Universidad Católica, Vicuña Mackenna 4860, Casilla 306, Santiago, Chile*
[2]*Facultad de Ciencias Astronómicas y Geofísicas, Universidad Nacional de La Plata, Paseo del Bosque S/N, B1900FWA, La Plata, Argentina*
[3]*Observatorio Astronómico, Universidad Nacional de Córdoba, Laprida 854, 5000 Córdoba, Argentina*

Accepted 2005 November 29. Received 2005 November 28; in original form 2005 August 05

ABSTRACT

Recently Splaver et al. have measured the masses of the white dwarf and the neutron star (NS) components of the PSR J1713+0747 binary system pair by means of the general relativistic effect known as Shapiro delay with very high accuracy. Employing these data we attempt to find the original configuration that evolved to the observed system. For this purpose we perform a set of binary evolution calculations trying to simultaneously account for the masses of both stars and the orbital period. In doing so, we considered normal (donor) stars with an initial mass of $1.5\,M_{\odot}$, while for the neutron star companion we assumed a mass of $1.4\,M_{\odot}$. We assumed two metallicity values for the donor star ($Z = 0.010$ and 0.020) and that the initial orbital period was nearly 3 d. In order to get a good agreement between the masses of the models and observations we had to assume that the NS is only able to retain $\lesssim 0.10$ of the matter transferred by the donor star. Calculations were performed employing the binary hydro code developed by Benvenuto & De Vito, that handles the mass transfer rate in a fully implicit way together with state-of-the-art physical ingredients and diffusion processes. Now our code also includes a detailed non-grey treatment for the atmospheres of white dwarfs (WDs).

We compare the structure of the resulting WDs with the characteristic age of PSR J1713+0747 finding a nice agreement with observations by Lundgren et al. especially for the case of a donor star with $Z = 0.010$. This result indicates that, at least for the purposes of this paper, the evolution of this kind of binary system is fairly well understood.

The models predict that, due to diffusion, the atmosphere of the white dwarf is an almost hydrogen-pure one. We find that such structures are unable to account for the colours measured by Lundgren et al. within their error bars. Thus, in spite of the very good agreement of the model with the main characteristics of the system, we find that some discrepancies in the WD emergent radiation remain to be explained.

Key words: binaries: general – stars: evolution – stars: white dwarfs.

1 INTRODUCTION

PSR J1713+0747 was discovered in a survey for millisecond pulsars (MSPs) with the 305-m Areceibo radio telescope (Foster, Wolszczan & Camilo 1993). It has been found that the pulsar has a spin period of 4.57 ms. Systematic changes in the apparent pulsar period have indicated the binary nature of this object. Foster et al. (1993) made the first determination of the binary model parameters of PSR J1713+0747. They found a nearly circular, 67.8-d binary orbit with a low-mass white dwarf (WD) companion. They estimated the companion mass via the mass function. Assuming the canonical value for the mass of the neutron star (NS) ($M_{\rm NS} = 1.4\,M_{\odot}$) they set a lower limit for the companion mass of $M_{\rm WD} \geqslant 0.28\,M_{\odot}$. Clearly, PSR J1713+0747 belongs to the family of NSs recycled by mass and angular momentum transfer from its normal (donor) companion (Alpar et al. 1982). This process leads to the formation of an MSP together with a cool WD companion. For a recent review on this kind of binary systems see Stairs (2004).

⋆E-mail: obenvenu@astro.puc.cl, obenvenuto@fcaglp.unlp.edu.ar (OGB); rohr@oac.uncor.edu (RDR); adevito@fcaglp.unlp.edu.ar (MADeV)
†Member of the Carrera del Investigador Científico, Comisión de Investigaciones Científicas de la Provincia de Buenos Aires (CIC), Argentina.
‡Member of the Carrera del Investigador Científico, Consejo Nacional de Investigaciones Científicas y Técnicas (CONICET), Argentina.
§Fellow of the CIC; Universidad Nacional de La Plata (UNLP); Instituto de Astrofísica de La Plata (CONICET).

PSR J1713+0747 has been continuously observed with an increasing degree of accuracy, which has been large enough to reveal the general relativistic effect known as Shapiro delay. This occurs due to a slight change in the arrival time of pulsar radiation due to the curvature of space near the WD companion of the MSP. According to general relativity, pulses are retarded as they propagate through the gravitational potential well of the WD. The first detection of Shapiro delay in PSR J1713+0747 is due to Camilo, Foster & Wolszczan (1994). They were able to set lower limits of the masses of the WD ($M_{\rm WD} > 0.27\,{\rm M}_\odot$) and NS ($M_{\rm NS} > 1.2\,{\rm M}_\odot$).

In a very recent work, Splaver et al. (2005) have reported the results of 12 yr of observations of PSR J1713+0747. The timing data yielded a large improvement in the measurements of the Shapiro delay that allowed for the determination of the individual masses for both components of the system. In principle, Shapiro delay yields $M_{\rm WD}$ and $\sin i$, where i is the inclination angle. In practice, unless $\sin i \sim 1$, Shapiro delay is highly covariant with $a_1 \sin i$[1] in the timing model fit and hence difficult to measure. Nevertheless, as shown by Splaver et al. (2005), in the case of PSR J1713+0747 Shapiro delay can be clearly distinguished. These high-precision detections allow for the masses of the pulsar and the companion star to be separately measured, being $M_{\rm NS} = 1.3 \pm 0.2\,{\rm M}_\odot$ and $M_{\rm WD} = 0.28 \pm 0.03\,{\rm M}_\odot$. These authors repeat the statistical analysis of timing solutions, now combined with the theoretical orbital period–core mass relation, and they obtain a larger mass for the NS: $M_{\rm NS} = 1.53^{+0.08}_{-0.06}\,{\rm M}_\odot$ (68 per cent confidence).

The pulsar masses in systems that evolve into pulsar–WD binaries are expected to be larger that those in NS–NS binaries (in the last case, the pulsar masses are expected within the range 1.25–1.44 $\rm M_\odot$). This is because the systems that evolve into pulsar–WD systems undergo extended periods of mass transfer. In a binary population study performed by Thorsett & Chakrabarty (1999), the authors find a narrow Gaussian distribution with a mean of $1.35\,{\rm M}_\odot$ and a width of $0.04\,{\rm M}_\odot$. The mass derived when the orbital period–core mass relation is imposed in PSR J1713+0747 implies a significantly heavier NS. Apart from PSR J1713+0747 there are other MSP plus WD systems for which it has been possible to measure the Shapiro delay and the masses of each component of the pair. One of them is PSR J0437−4715 (van Straten et al. 2001) for which $M_{\rm WD} = 0.236 \pm 0.017\,{\rm M}_\odot$, and $M_{\rm NS} = 1.58 \pm 0.18\,{\rm M}_\odot$. The other is PSR B1855+09 for which $M_{\rm WD} = 0.258^{+0.028}_{-0.016}\,{\rm M}_\odot$ and $M_{\rm NS} = 1.50^{+0.26}_{-0.14}\,{\rm M}_\odot$ for the pulsar mass (Kaspi, Taylor & Ryba 1994). The uncertainties on all these measurements are large and the question of the distribution of pulsar masses in these systems remains open.

One very important parameter is the characteristic age of the pulsar $\tau_{\rm PSR}$. The age of a spin-down powered pulsar is given by

$$\tau_{\rm PSR} = \frac{P}{(n-1)\dot{P}}\left[1 - \left(\frac{P_0}{P}\right)^{n-1}\right], \qquad (1)$$

where P is the pulsar period, $\dot{P}$ the temporal derivative of the period, P_0 is the initial period and n the braking index. For magnetic dipole radiation we have $n = 3$, and if we assume $P_0 \ll P$, the pulsar spin-down age is given by $\tau_{\rm PSR} = P/(2\dot{P})$, the 'characteristic age' of the pulsar. The uncertainty in the pulsar age is caused by n and P_0. On the other hand, the transverse velocity of the pulsar causes an apparent acceleration that contributes to the observed period derivative. Ignoring this latter effect can lead to erroneous estimations of the characteristic pulsar age. Splaver et al. (2005) found for PSR J1713+0747, $\tau_{\rm PSR} = 8$ Gyr. Using the restrictions for the mass of the WD in this system, Hansen & Phinney (1998) obtain cooling ages in the range 6.3–6.8 Gyr, but if they consider the dispersion measure distance estimates, they can obtain cooling ages up to 13.2 Gyr.

If the pulsar has a close companion WD, we expect the cooling age for the WD to approximately match the age of the pulsar. For the kind of systems we are here interested in, $\tau_{\rm PSR}$ should correspond to the age of the helium WD (hereafter He WD) counted since the end of the main (initial) Roche lobe overflow (RLOF) episode. This is so because the initial RLOF is the only one able to transfer the amount of matter needed to spin up the NS ($\approx 0.1\,{\rm M}_\odot$). As we shall show below, models of normal stars leading to the formation of the WD companion suffer from at least one hydrogen thermonuclear flash leading to a supplementary RLOF. However, these flash-driven RLOFs are not relevant in spinning up the NS because of the tiny amount of transferred matter (Benvenuto & De Vito 2004). Because of these reasons, the WD in PSR J1713+0747 should have spent a time of $\tau_{\rm PSR} \approx 8$ Gyr since the end of the main RLOF episode.

The aim of this work is to test the present status of the theory of stellar evolution in binary systems by computing a set of evolutionary tracks in order to reproduce the main characteristics of the PSR J1713+0747 system, particularly the masses of the components, the orbital period and the characteristic time-scale for the cooling of the WD. In our opinion this is an interesting problem because of the high precision of the measurements performed for the system we are dealing with.

The WD companion of PSR J1713+0747 has been detected by Lundgren, Foster & Camilo (1996) with *Hubble Space Telescope* (*HST*) observations (see Table 1). This fact provides us with the interesting possibility of confronting theory with observations. In doing so we shall employ the available observational data of the WD in PSR J1713+0747 as a test of the accuracy of our evolutionary calculations and *not* as the main data to account for. We shall do so because of two reasons. First, we judge that the accuracy of the radioastronomical measurements of the system is so high that they should be considered as the fundamental quantities for this problem. Secondly, this procedure is interesting in order to gauge the ability of the binary stellar evolution theory combined with atmosphere models in predicting the characteristics of a WD and to evaluate the possibility of helping for a first optical detection of WDs as companions of MSPs.

Regarding the viability of this procedure, we should quote that recently, Benvenuto & De Vito (2005) have been able to account

Table 1. Main characteristics of the WD component of the PSR J1713+0747 system, taken from Lundgren et al. (1996). The numbers in parentheses represent the uncertainty in the last digits quoted.

Quantity	Measured value
m_B	>27.1
m_V	26.0(2)
m_I	24.1(1)
$B - V$	>1.1
$V - I$	1.9(2)
$m - M$	10.2(5)
E_{B-V}	0.08(2)

[1] a_1 is the orbital semimajor axis.

for the masses, orbital period and characteristics evolutionary timescales of the WDs in PSR J0437−4715 and PSR B1855+09.

Our particular interest on this type of systems has been focused on to the study of low-mass He WDs (see Benvenuto & De Vito 2004, 2005). Besides, these systems are appropriate for testing our evolutionary models of cooling He WDs.

The remainder of the paper is organized as follows. In Section 2, we present the numerical code we have employed. In Section 3, we describe the evolutionary results we have found for the PSR J1713+0747 binary system. Finally, in Section 4 we discuss the implicates of our calculations and summarize the main conclusions of this work.

2 THE NUMERICAL CODE

The binary stellar evolution calculations presented below have been performed employing the stellar code described in Benvenuto & De Vito (2004) now with a non-grey model atmosphere as detailed in Rohrmann (2001). We briefly mention that our code employs a generalized Henyey technique that allows for the computation of mass transfer episodes in a fully implicit way (Benvenuto & De Vito 2003). The code has an updated description of opacities, equation of state, nuclear reactions and diffusion while we simultaneously compute orbital evolution considering the main processes of angular momentum loss: angular momentum carried away by the matter lost from the system, gravitational radiation and magnetic braking. To be more specific, in accounting for the magnetic braking we follow Podsiadlowski, Rappaport & Pfahl (2002) and incorporate equation (36) of Rappaport, Verbunt & Joss (1983), assuming $\gamma = 4$. We neglect irradiation of the donor star by the MSP.

In our treatment of the orbital evolution of the system, we shall consider that the NS is able to retain a fraction β of the material coming from the donor star: $\dot{M}_{\rm NS} = -\beta\dot{M}$ (where $\dot{M}_{\rm NS}$ is the accretion rate of the NS and $\dot{M}$ the mass transfer rate from the normal star). β should be considered as a free parameter, because at present it is not possible to compute it from first principles.[2] For simplicity, it will be considered as a constant throughout all the RLOF episodes. We shall assume that the material lost from the binary system carries away the specific angular momentum of the compact object.

In our previous works on binary evolution we have considered grey atmospheres. Now, for a proper treatment of the cooling behaviour of the WD companion of the MSP, we have incorporated detailed non-grey model atmospheres as an outer boundary condition for evolutionary models of the WD. The use of non-grey atmospheres for this purpose is particularly important in the late stages of He WD cooling (Serenelli et al. 2001). Besides, the atmosphere code allows us to determine the emergent flux from the WD and to interpret its magnitudes and colours.

The procedures employed in the calculation of local thermodynamic equilibrium model atmospheres are basically the same as described in Rohrmann (2001) and Rohrmann et al. (2002). Models are computed assuming hydrostatic and radiative–convective equilibrium. Convective transport is treated within the mixing-length theory. We include line blanketing by Lyman lines of hydrogen and helium, and the pseudo-continuum opacity from the Balmer and Paschen edges. Collision-induced absorption (CIA) becomes an important source of infrared opacity in WDs cooler than $T_{\rm eff} \approx$ 5000 K. Our code includes a detailed description of CIA due to H_2–H_2 (Borysow, Jorgensen & Fu 2001), H_2–He (Jorgensen et al. 2000) and H–He (Gustafsson & Frommhold 2001). Chemical equilibrium is based on the occupation probability formalism as described in Rohrmann et al. (2002), and includes H, H_2, H^+, H^-, H_2^+, H_3^+, He, He^-, He^+, He^{2+}, He_2^+ and HeH^+. Ionic molecules He_2^+ and HeH^+ were incorporated recently (for details, see Gaur et al. 1988 and Harris et al. 2004). We also added the continuous absorption opacity of He_2^+ following Stancil (1994).

In order to optimize the numerical effort, initially we shall compute the evolutionary sequences employing grey atmospheres. In this way, we search for the correct configuration for the binary system able to account for the main characteristics of the binary system (masses, orbital period and characteristic age). After identifying a plausible configuration, we have at hand a complete evolutionary track from the zero-age main-sequence (ZAMS) up to the end of the WD cooling sequence. Then we rerun the code, now including the non-grey stellar atmosphere. In doing so, we shall start this detailed computation from the top of the last cooling track, near the conditions in which the star has its absolute maximum effective temperature. In this way, we avoid computing a full evolutionary track with a non-grey atmosphere without missing relevant detail of the physics of the problem we are interested in. This is very important in order to keep the numerical computations affordable.

3 RESULTS

In order to account for the main characteristics of the PSR J1713+0747 binary system we have computed a set of evolutionary models. As stated above, our primary quantities are the masses and orbital period and the observed WD conditions are employed as a test of how plausible is the theory of binary stellar evolution we are employing. For this purpose we have to set values for many initial parameters. We shall assume the initial mass of the normal component of the pair to be $1.5\,{\rm M}_\odot$ while for the NS we employ its 'canonical value' of $M_{\rm NS} = 1.4\,{\rm M}_\odot$. Here, we shall consider two values for the metallicity of the normal star: $Z = 0.010$ and 0.020.

Regarding mass transfer, we have assumed that $\dot{M}_2 = -\beta\dot{M}_1$ where subindex 1 (2) corresponds to the normal (neutron) star. As β is constant, this implies that $M_2 + \beta M_1 = M_2^{\rm i} + \beta M_1^{\rm i}$ where superscript (i) indicates that these are initial masses. Immediately we find $\beta = (M_2 - M_2^{\rm i})/(M_1^{\rm i} - M_1)$. If we assume that the NS has accreted $\lesssim 0.1\,{\rm M}_\odot$, then $\beta \lesssim 0.10$. Hereafter, we shall adopt the upper limit value of $\beta = 0.10$.

After considerable search in the parameter space we found two plausible solutions. These are a pair with the above-mentioned masses, a metallicity of $Z = 0.010$ and an initial period $P_{\rm i} = 3.05\,{\rm d}$ and another with $Z = 0.020$ and an initial period $P_{\rm i} = 3.10\,{\rm d}$. From here on, we shall explore the evolution of these systems and its comparison with observations. While we have not performed (a very time-consuming) finer exploration in the parameter space, we interpret that these two systems are suitable for our purposes. In any case it is worth mentioning that significantly lower-mass values for the donor star would require times in excess of the Hubble time in order to get a dim WD object like the one observed for the system we are studying here. Also, longer initial periods would force the system to undergo a common envelope episode because at the onset of the RLOF, the donor star would have a very deep outer convective zone (hereafter OCZ) and consequently to a considerable shrinkage of the orbit.

We decided not to explore in detail the possibility of a lower value for the metallicity. As it will be clear below, the systems we have

[2] For the cases of PSR J0437−4715 and PSR B1855+09, in order to account for the characteristics of each of these systems, it has been found (Benvenuto & De Vito 2005) that β should be $\lesssim$0.12.

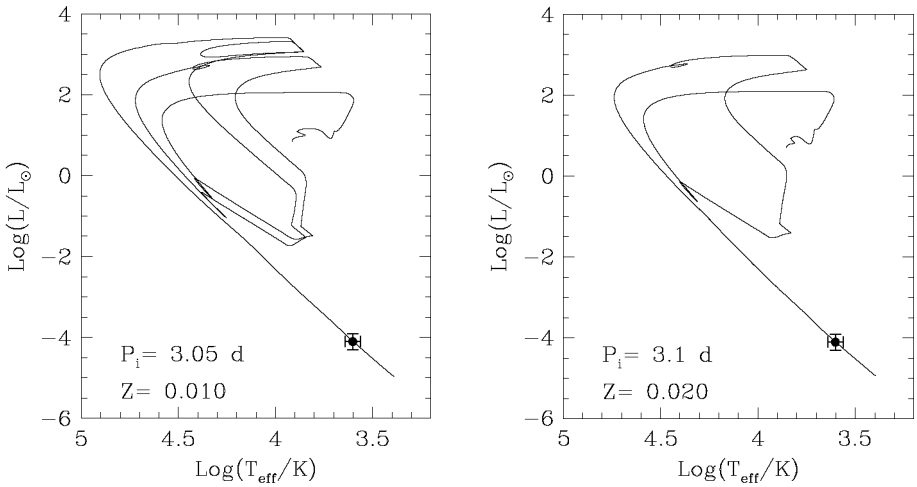

Figure 1. Evolutionary tracks for stars with an initial mass of 1.50 $M_\odot$ as companions of an NS with a canonical mass value of 1.4 $M_\odot$. Left-hand panel corresponds to the case of an abundance of $Z = 0.010$ and an initial period of 3.05 d. Right-hand panel corresponds to the case of solar chemical composition and an initial period of 3.10 d. For the case of $Z = 0.010$ the star undergoes two hydrogen thermonuclear flashes while for $Z = 0.020$ the object experiences only one. For comparison, we also include the luminosity and effective temperature for the WD in the PSR J1713+0747 as deduced from our models with a solid circle with its corresponding error bars. See text for further details.

chosen produce WD objects with mass values compatible with the (1σ) error bar but almost in its upper limit. If we look for values of $Z < 0.010$ we would find a larger final WD mass as it is clear from the mass–period relation given by Nelson, Dubeau & MacCannell (2004)

$$\log\left(\frac{P_{\rm f}}{1\,{\rm d}}\right) = 10.7\left(\frac{M_{\rm f}}{{\rm M}_\odot}\right) + 0.3\log Z - 0.98277. \qquad (2)$$

Thus, for lower Z-values from the ones considered here we would find WD masses in excess from the observed error bars. This result suggests that a metallicity lower than $Z \lesssim 0.010$ is unlikely.

The evolutionary tracks followed by the normal star of the system are shown in Fig. 1 for each metallicity value considered here. In both cases the star completes its core hydrogen burning, evolves to the red giant branch and develops an OCZ. In these conditions the star overflows its Roche lobe which corresponds to the onset of the initial mass transfer episode. In Fig. 2, we show the evolution of the period of the system as a function of the masses of the components of the pair. For both cases the mass of the donor star finally falls inside the 1σ error bar. For the case of the NS, its final mass is slightly larger than the one found by Splaver et al. (2005) but inside the error bar of the allowed mass interval if a theoretical mass–radius relation is considered. In view of its present large uncertainty, we shall consider the mass value for the NS as acceptable.

It is important to remark that, in both cases we have found that during the initial RLOF the mass transfer is stable and the system does not suffer from a common envelope episode (see Podsiadlowski et al. 2002 and Benvenuto & De Vito 2005 for similar results). After the RLOF the star contracts and diffusion carries hydrogen inwards up to the point at which the bottom of the hydrogen envelope is hot enough to ignite hydrogen in semidegenerate conditions (Althaus, Serenelli & Benvenuto 2001). Then a thermonuclear flash occurs. In the case of $Z = 0.010$ the star undergoes two flashes while for $Z = 0.020$ the object experiences only one. After flashes the star cools down as a He WD with an outermost layer rich in hydrogen. For further details see, e.g. Benvenuto & De Vito (2004, 2005) (see also Sarna, Ergma & Gerskevits-Antipova 2000 and Nelson et al. 2004). The main characteristics of the WD final cooling tracks are

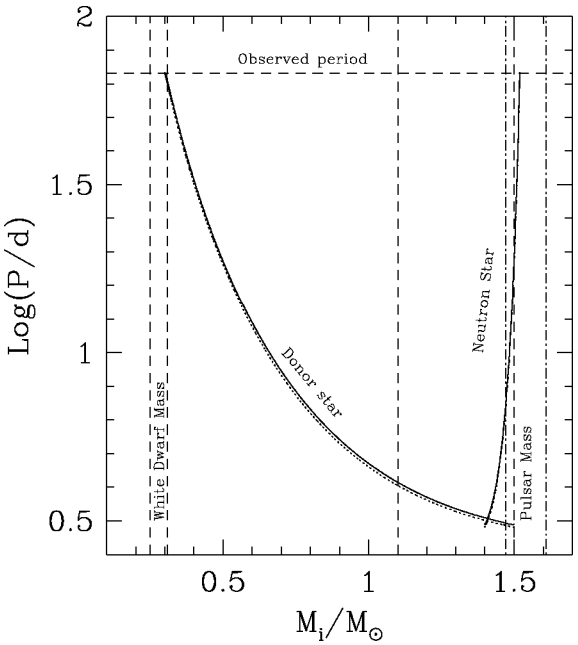

Figure 2. Mass versus period for the evolutionary sequences shown in Fig. 1. Dotted lines represent the case of the system with 1.50 $M_\odot$, a metallicity of $Z = 0.010$ and an initial period of $P_{\rm i} = 3.05$ d. Meanwhile, solid lines stand for the case of the same initial mass but a metallicity of $Z = 0.020$ and an initial period of $P_{\rm i} = 3.10$ d. Vertical short dashed lines on the left-hand side represent the observed mass of the WD companion with its corresponding error, while the vertical short dashed lines on the right-hand side correspond to the mass of the NS also with its error bar. The other estimation of the NS mass derived employing the orbital period–core mass relation (see Section 1) is shown with vertical dot–short dashed lines. The horizontal long dashed line represents the observed orbital period (known with a very large degree of accuracy). The conditions considered for an evolutionary sequence to be acceptable to account for the characteristics of the PSR J1713+0747 system are that both final masses (of the WD and NS, respectively) must be inside the error bars and reach the observed orbital period.

Table 2. Selected evolutionary stages for the system with a metallicity of $Z = 0.010$, initial period of 3.05 d. We tabulate the age, effective temperature, logarithm of the luminosity, logarithm of the central temperature, logarithm of the central density, the mass fraction embraced in the OCZ, the fractional amount of hydrogen in the whole star, the gravitational acceleration at the stellar surface, absolute visual magnitude, colour indices and the BC. Quantities without specified units are given in CGS. The final mass and orbital period values for this system are $M_{\rm f} = 0.299\,4507\,{\rm M}_{\odot}$ and $P_{\rm f} = 68.288$ d, respectively.

Age (Gyr)	$T_{\rm eff}$	$\log(L/{\rm L}_{\odot})$	$\log T_{\rm C}$	$\log\rho_{\rm C}$	$10^3\,q_{\rm OCZ}$	$10^4\,M_{\rm H}/M_*$	$\log g$	M_V	BC
	$(U-B)$	$(B-V)$	$(V-R)$	$(V-K)$	$(R-I)$	$(J-H)$	$(H-K)$	$(K-L)$	
2.245	10772	−2.167	7.263	5.647	0.000	7.492	7.165	10.582	
	−0.404	0.060	0.010	−0.143	0.004	0.047	−0.116	−0.036	−0.413
2.425	9424	−2.439	7.160	5.662	0.000	7.473	7.205	11.124	
	−0.452	0.140	0.083	0.153	0.083	0.090	−0.097	−0.033	−0.274
2.872	7622	−2.858	6.999	5.678	0.001	7.450	7.256	12.062	
	−0.517	0.280	0.201	0.698	0.206	0.178	−0.059	−0.012	−0.166
3.515	6301	−3.223	6.866	5.687	0.016	7.430	7.290	12.924	
	−0.390	0.451	0.312	1.221	0.319	0.267	−0.011	0.035	−0.114
5.515	4812	−3.756	6.659	5.697	9.747	7.406	7.355	14.450	
	0.060	0.798	0.523	2.071	0.525	0.366	0.057	0.170	−0.308
8.001	4184	−4.021	6.480	5.702	9.747	7.405	7.377	15.234	
	0.233	0.968	0.631	2.085	0.632	0.138	−0.021	0.387	−0.430
10.118	3750	−4.220	6.349	5.705	7.303	7.407	7.385	15.684	
	0.302	1.067	0.690	1.558	0.677	−0.176	−0.167	0.763	−0.382
14.967	2995	−4.620	6.109	5.709	3.907	7.406	7.395	16.337	
	0.489	1.223	0.700	0.181	0.480	−0.386	−0.438	1.738	−0.035
19.919	2502	−4.936	5.935	5.710	1.853	7.405	7.399	16.768	
	0.654	1.331	0.594	−0.876	−0.065	−0.269	−0.734	2.557	0.324

Table 3. Selected evolutionary stages for the system with a metallicity of $Z = 0.020$, initial period of 3.10 d. Columns have the same meaning as in Table 2. The final mass and orbital period values for this system are $M_{\rm f} = 0.303\,3765\,{\rm M}_{\odot}$ and $P_{\rm f} = 67.762$ d, respectively.

Age (Gyr)	$T_{\rm eff}$	$\log(L/{\rm L}_{\odot})$	$\log T_{\rm C}$	$\log\rho_{\rm C}$	$10^3\,q_{\rm OCZ}$	$10^4\,M_{\rm H}/M_*$	$\log g$	M_V	BC
	$(U-B)$	$(B-V)$	$(V-R)$	$(V-K)$	$(R-I)$	$(J-H)$	$(H-K)$	$(K-L)$	
3.191	10582	−2.176	7.194	5.673	0.000	16.696	7.150	10.579	
	−0.404	0.070	0.018	−0.110	0.013	0.052	−0.114	−0.036	−0.387
3.542	9141	−2.480	7.066	5.686	0.000	16.428	7.199	11.203	
	−0.466	0.159	0.100	0.227	0.102	0.100	−0.093	−0.031	−0.253
4.010	8104	−2.721	6.969	5.694	0.001	16.194	7.230	11.745	
	−0.514	0.238	0.168	0.537	0.172	0.150	−0.071	−0.021	−0.192
5.059	6895	−3.035	6.863	5.701	0.006	15.868	7.264	12.467	
	−0.478	0.362	0.256	0.966	0.263	0.226	−0.036	0.008	−0.128
7.054	5778	−3.376	6.772	5.706	0.140	15.531	7.298	13.323	
	−0.260	0.557	0.374	1.483	0.380	0.301	0.020	0.069	−0.132
10.272	4713	−3.788	6.635	5.713	11.219	15.300	7.356	14.558	
	0.090	0.826	0.541	2.116	0.543	0.364	0.044	0.194	−0.336
15.114	3707	−4.235	6.330	5.719	7.882	15.274	7.386	15.712	
	0.320	1.077	0.695	1.480	0.678	−0.202	−0.192	0.818	−0.372
20.711	2851	−4.701	6.072	5.723	3.363	15.257	7.396	16.444	
	0.535	1.254	0.679	−0.106	0.363	−0.368	−0.507	1.959	0.061
24.505	2520	−4.918	5.944	5.724	1.923	15.257	7.399	16.737	
	0.647	1.326	0.599	−0.828	−0.038	−0.273	−0.713	2.517	0.309

given in Tables 2 and 3 for the cases of $Z = 0.010$ and 0.020, respectively.

In Fig. 3, we show the luminosity of the models as a function of the age counted since the end of the initial RLOF. Notice that, in spite of the fact that the masses of the WDs of both considered cases are very similar, there is an important difference regarding the cooling of the models. As models with $Z = 0.010$ evolve faster than those with $Z = 0.020$, the WD is predicted to be fainter. Specifically, at the characteristic age of the MSP, for the case of the evolutionary track with $Z = 0.010$ ($Z = 0.020$) the WD has a luminosity of $\log(L/{\rm L}_{\odot}) = -4.210(-3.825)$. In Fig. 4, we show the evolution of the absolute visual magnitude as a function of the age of the star counted since the beginning of core hydrogen burning.

In Fig. 5, we show the final mass–orbital period relation for low-mass He WDs in orbit with MSPs including the one in PSR J1713+0747 system and the other well-determined cases (in PSR J0437−4715 and PSR B1855+09 systems) together with some recent calculations by Sarna et al. (2000), Podsiadlowski et al. (2002), Nelson et al. (2004) and Benvenuto & De Vito (2005), and also the relations given by Rappaport et al. (1995) and Nelson et al. (2004). The WD in PSR J1713+0747 system is the most massive among the three accurately measured WDs of this type. While the mean value

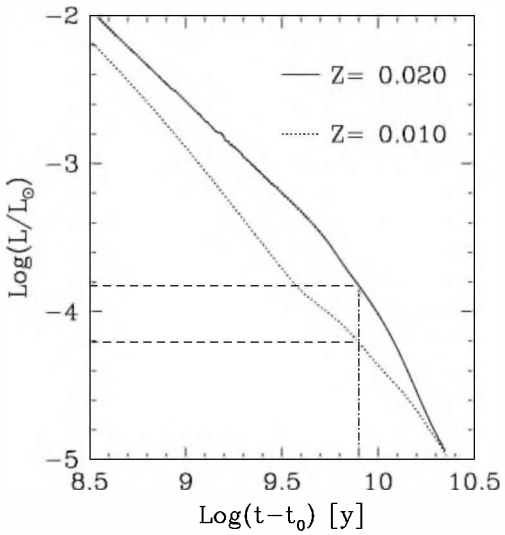

Figure 3. Evolution of luminosity as a function of time counted since the end of the initial mass transfer episode. Solid and dotted lines have the same meaning as in Fig. 2. The vertical dot–short dashed line represents the characteristic time-scale of the MSP which, because of evolutionary reasons, should correspond to the present conditions of the He WD. Horizontal short dashed lines stand for the luminosity the WD should have at the characteristic age of the pulsar.

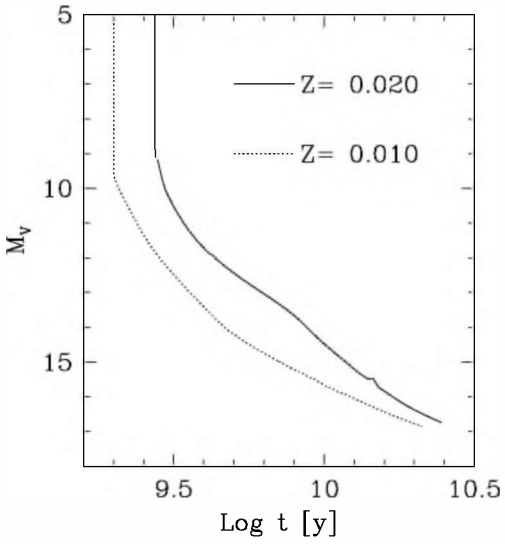

Figure 4. The evolution of the absolute visual magnitude as a function of the age of the star counted from the ZAMS on.

of $M_{\rm WD} = 0.28\,{\rm M}_\odot$ is marginally compatible with the available calculations, the 1σ value of $M_{\rm WD} = 0.31\,{\rm M}_\odot$ is in nice agreement with previous computations as well as with those performed in this paper.

Having determined the possible evolutionary sequences followed by the normal, donor star in PSR J1713+0747 binary system, we are in a position to analyse the observational appearance of the last contraction towards the WD regime. In Figs 6 and 7, we show the computed $((B-V),(V-I))$ colour–colour and $(M_V,(V-I))$ magnitude–colour diagrams. Observations of cool WDs (symbols) have been plotted for comparison. The cooling curves at $Z = 0.010$ (dotted lines in Figs 6 and 7) and $Z = 0.020$ (solid lines in the same figures) are essentially identical because both tracks

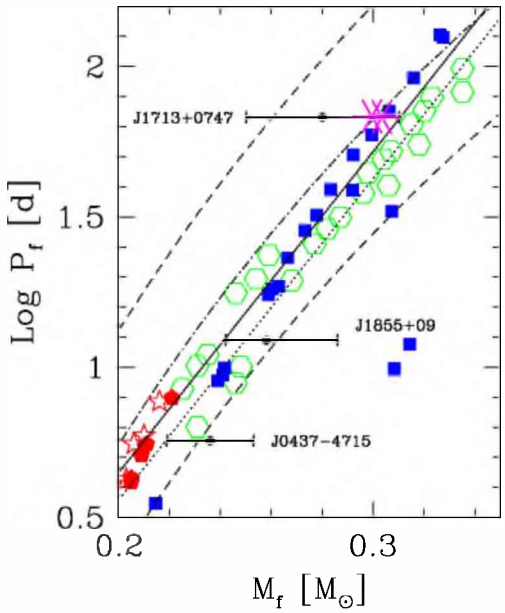

Figure 5. The mass versus orbital period relation for He WDs and the WD in PSR J1713+0747 system. Starred hexagons denote the two cases considered here that account for the characteristics of the system we are studying here. Solid (dotted) line denotes the relation predicted by Nelson et al. (2004) for a metallicity value of $Z = 0.020$ ($Z = 0.010$). Dot–short dashed line depicts the relation given in Rappaport et al. (1995) together with its uncertainty, shown by short dashed lines. Filled squares, green hollow hexagons, hollow stars and filled pentagons stand for data from Benvenuto & De Vito (2005) (for $Z = 0.020$); Podsiadlowski et al. (2002) (for $Z = 0.020$) and Sarna et al. (2000) (for $Z = 0.020$ and 0.010, respectively) . We also include the other two accurately measured masses (in PSR J0437−4715 and PSR B1855+09 systems) of low-mass WDs in binary systems together with MSPs.

correspond to very similar stellar masses ($M = 0.302\,{\rm M}_\odot$ within 1 per cent) and atmospheric composition. The main difference between the two evolutionary solutions arises from the cooling ages (labels on the plots).

Since gravitational settling dominates the chemical stratification after a relatively short cooling time (typically 0.1 Myr), evolutionary calculations predict that the WD has mostly hydrogen floating at its visible surface (photosphere). The formation of molecular hydrogen becomes important as the star cools down. The H_2 CIA opacity is very strong in the infrared and largely determines the shape of the spectral energy distribution for cool WD models. As a consequence of the molecular opacity, the $(V-I)$ colour becomes bluer when the effective temperature falls below 3600 K. The turnoff of the WD cooling sequences is located at $(V-I) \approx 1.4$, with $M_V \approx 15.8$ and $(B-V) \approx 1.1$.

As stated in Section 1, optical observations of the pulsar companion have been carried out by Lundgren et al. (1996) (see Table 1). The timing parallax distance of 1.1 ± 0.1 kpc yields a distance modulus $m - M = 10.2 \pm 0.2$. If we adopt an interstellar absorption of $A_V = 0.1$ as a conservative estimate (Burstein & Heiles 1982), the absolute visual magnitude of the pulsar companion is $M_V = 15.7 \pm 0.4$. Thus, the observed companion is located near the turnoff of the evolutionary sequences (where $T_{\rm eff} \approx$ 3600 K) although appears redder in the $(V-I)$ colour (see Figs 6 and 7). Unfortunately, multicolour optical observations only provide a lower limit for $(B-V)$ colour such that it offers a relatively poor constraint. The observed $(V-I)$ colour is $\approx$0.4 mag redder than the cooling sequences. It is worth noting that, due to the CIA

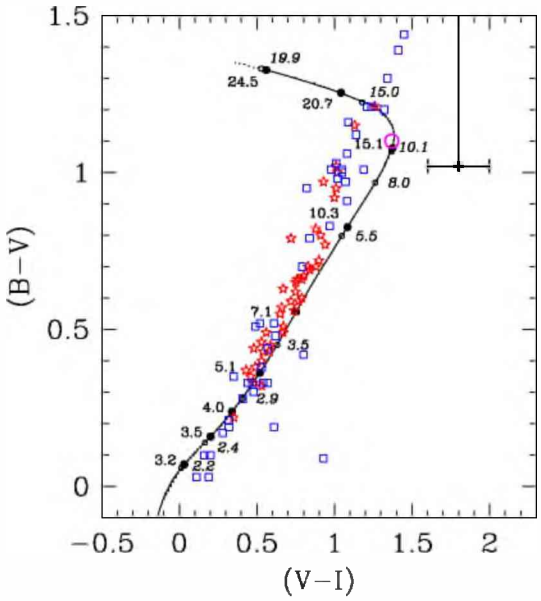

Figure 6. The evolutionary tracks of the models considered in this paper as representative of the WD in PSR J1713+0747 system in the $(B-V)$ versus $(V-I)$ plane. The dotted (solid) line stands for the results with $Z = 0.010$ ($Z = 0.020$). Actually both models yield very similar colour–colour curves. Solid circles represent the conditions for the case of $Z = 0.020$ given in Table 3 for which labels to the left-hand side are their ages (in Gyr). Hollow circles stand for the conditions corresponding to the case of $Z = 0.010$ given in Table 2 for which labels to the right-hand side (in italics) are their ages (in Gyr). The best fit corresponding to the WD in PSR J1713+0747 system is shown with an open circle located approximately at $(B-V) = 1.1$ and $(V-I) = 1.4$, while the observational data given in Lundgren et al. (1996) is shown with a solid dot with its corresponding error bars. For comparison, we have also included data corresponding to DA and non-DA WDs (denoted with hollow stars and hollow squares) given by Bergeron et al. (2001) and McCook & Sion (1987). The value of $(B-V)$ corresponding to the best fit is compatible with the lower limit given by Lundgren et al. (1996); however $(V-I)$ is too high for hydrogen atmospheres.

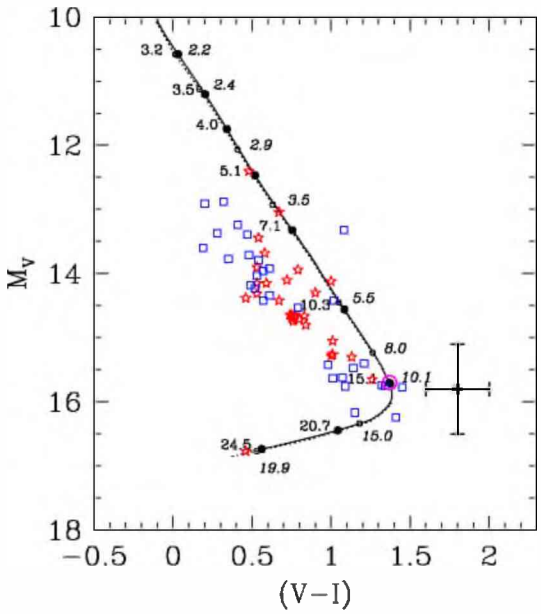

Figure 7. The evolutionary tracks of the models considered in this paper as representative of the WD in PSR J1713+0747 system in the $(V-I)$ versus M_V plane. Lines, labels and symbols have the same meaning as in Fig. 6. Notice that, while the M_V is very well accounted for by our models, $(V-I)$ is far higher than the values predicted by almost pure hydrogen atmospheres.

opacity, $(V-I) \approx 1.5$ represents an extreme upper limit for WDs with hydrogen-rich atmospheres (e.g. Rohrmann et al. 2002). It is therefore somewhat disturbing that the $(V-I)$ index observed by Lundgren et al. (1996) is too red compared with rich-hydrogen envelope predictions. The origin of this discrepancy is unknown. It could be due to a missing opacity source in the WD atmosphere itself or a non-hydrogen-rich composition. Additional observations are necessary to disentangle this issue.

We can convert the observed magnitudes (m) into fluxes (f_λ^m) and compare the resulting energy distributions with those predicted from our model atmosphere calculations. The average flux and the magnitude for each passband is related in the form

$$m = -2.5 \log f_\lambda^m - c_m \,,$$

with c_m being a calibration constant. The Eddington flux at the stellar surface H_λ^m is evaluated from the relation

$$f_\lambda^m = 4\pi \left(\frac{R}{D}\right)^2 H_\lambda^m$$

where R/D is the ratio of the radius of the star to its distance from the Earth. We use the filter transmission curves given in Bessell (1990), the parallax distance of $D = 1.1 \pm 0.1$ kpc (from pulsar timing), averaged values of the interstellar extinction (Burstein & Heiles 1982), and the radius derived from our evolutionary models $R = (1.90 \pm 0.05) \times 10^{-2}\,\mathrm{R}_\odot$ (over a range of temperatures $T_{\rm eff} < 5000$ K).[3] The computed fluxes are shown in Fig. 8. These values confirm that the binary companion apparently exhibits a strong infrared flux *excess* (or a blue deficiency).

The photometric spectrum was fitted using the evolutionary sequences at $Z = 0.010$ and 0.020 (their surface gravities differ by less than 0.1 per cent for the temperature range of interest). The results are presented in Fig. 8 and listed in Table 4. A good fit to the energy distribution of the WD companion cannot be achieved with a unique effective temperature. The flux at the V band can be represented by a model with $T_{\rm eff} = 3670 \pm 280$ K, which also fits the upper limit detected for the B band. However, for the I filter we obtain $T_{\rm eff} = 4320 \pm 180$ K. These solutions, which differ quantitatively by 650 K, fall within the range of previous temperature evaluations: $T_{\rm eff} = 3700 \pm 100$ K [Lundgren et al. 1996, based on a temperature calibration of $(V-I)$ colour determined by Monet et al. 1992], $T_{\rm eff} = 3430 \pm 270$ K (Hansen & Phinney 1998, based on blackbody fits to *HST* data) and $T_{\rm eff} = 4250 \pm 250$ K (Schönberner, Driebe & Blöcker 2000, from evolutionary WD models).

The relation between photometric data and effective temperature of the WD can be appreciated in Fig. 9. There, broad-band colours and absolute visual magnitude of the observed star (dashed vertical lines) are compared with predictions from present evolutionary calculations (solid line), blackbody approximation (dotted line), and pure helium broad-band colours of Bergeron, Saumon & Wesemael (1995) for $\log g = 7.0$ and 7.5 (dashed lines). Absolute magnitudes derived for helium models were evaluated using a radius of $R = 1.9 \times 10^{-2}\,\mathrm{R}_\odot$ and bolometric corrections (BCs) provided by those authors. The $(V-I)$ broad-band colour yields a temperature estimate of 3450 K when a blackbody spectrum is assumed, which

[3] The WD radius is nearly constant at advanced cooling stages.

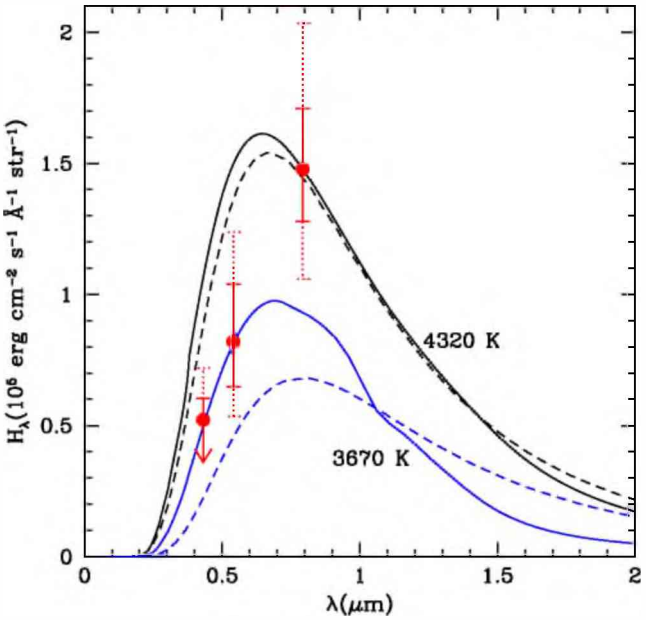

Figure 8. Energy distribution of WD model atmospheres with $T_{\rm eff} = 4320$ and 3670 K (continuous lines) and the blackbody spectra at these temperatures (dashed lines). The photometric observations are represented by filled circles. Continuous error bars include uncertainties in stellar radius and photometric data only. Dotted error bars includes the parallax error also.

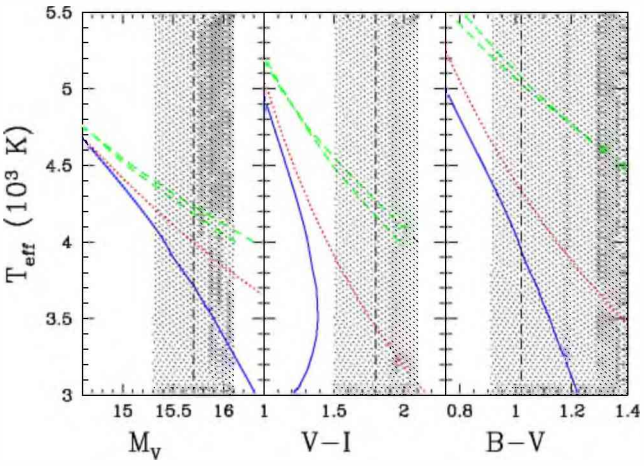

Figure 9. Effective temperature versus absolute magnitude and colours. Solid lines denotes the cooling WD track with hydrogen-rich atmospheres predicted for the MSP companion. The solid $V - I$ curve turns to the left-hand side at low temperatures due to the molecular hydrogen opacity. Dotted lines represent blackbody solutions, and dashed lines correspond to helium-pure atmosphere at $\log g = 7.0$ and 7.5 taken from Bergeron et al. (1995). Vertical dashed lines correspond to the observed values for the companion of pulsar J1713+0747 (the WD absolute magnitude is based on the distance inferred from the dispersion measure). We denote with a shaded area the range compatible with the photometric data.

is considerably lower than the temperature derived from the M_V fit ($\approx$4000 K). Hydrogen-rich atmospheres of WDs deviate strongly from the blackbody approximation at low $T_{\rm eff}$ as the opacities become dominated by molecular hydrogen. The observed $(V - I)$ colour is far off the hydrogen sequence as shown in Fig. 9 (middle panel), whereas the M_V fit indicates a temperature of approximately 3700 K. On the other hand, the observed *BVI* magnitudes can be understood with a helium-pure atmosphere if $T_{\rm eff} \approx 4250 \pm 300$ K. All cases fall within the limit observed for the $(B - V)$ colour.

This exercise shows that the effective temperature of the WD companion of PSR J1713+0747 should be between 3700 and 4300 K. Taking into account the uncertainties in the photometric data fits, we finally adopt $T_{\rm eff} = 4000 \pm 400$ K as a conservative solution based on *HST* observations. Consequently, using the $T_{\rm eff}$–radius relation of our evolutionary calculations, we determine a luminosity in the range $-3.92 > \log(L/{\rm L}_\odot) > -4.29$. As shown in Fig. 1, the detected optical counterpart lies on the calculated cooling tracks. Furthermore, for the case of $Z = 0.010$ the cooling age deduced from our models is 9 ± 2 Gyr. If we consider that the star ends its initial RLOF with an age of 1.99 Gyr, we find that the WD has spent 7 ± 2 Gyr in evolving since detachment, which is in excellent agreement with the pulsar's characteristic age! However, for $Z = 0.020$ our models indicate that the star needs 13.5 ± 2 Gyr in evolving up to the present stage. For this metallicity, detachment occurs at 2.73 Gyr. Then, the star would have needed 10.8 ± 2 Gyr to cool which is a larger time-scale than the characteristic age of the pulsar.

Table 4. WD model atmospheres for the optical observations by Lundgren et al. (1996).

$T_{\rm eff}$ (K)	$\log(L/{\rm L}_\odot)$	$\log g$	M_V	$(B - V)$	$(V - I)$	BC
4320	−3.95	7.373	15.032	0.932	1.218	−0.415
3670	−4.23	7.387	15.689	1.085	1.377	−0.364

This fact indicates that the donor star very likely has a metallicity $Z \approx 0.010$.

4 DISCUSSION AND CONCLUSIONS

In this paper, we have computed a set of binary evolutionary tracks in order to account for the main characteristics of the PSR J1713+0747 system. We did so with a binary stellar evolution code including a non-grey treatment of the atmospheric layers.

Thanks to the high accuracy of the timing of this MSP, it has been possible to measure the general relativistic Shapiro delay effect to derive separate values for the masses of the WD and the NS. Starting out from this fact, we performed a numerical experiment in which we computed the full evolution of the system in order to account for the masses and orbital period of the system and *then* considered the evolutionary status of the WD. Notice that the pulsar should have a characteristic age equal to the age of the WD counted since the end of the initial RLOF (see Section 1 for further details). Thus, at the characteristic age of the pulsar, the WD should resemble the object observed by Lundgren et al. (1996).

We found that a system with initial masses of $M = 1.5\,{\rm M}_\odot$, $M_{\rm NS} = 1.4\,{\rm M}_\odot$ for the normal (donor) star and NSs (respectively) in which the NS is able to accrete a fraction $\beta = 0.10$ of the transferred mass (the mass lost from the system is assumed to carry away a specific angular momentum equal to that of the NS) accounts for the PSR J1713+0747 system if $Z = 0.010$ and $P_{\rm i} = 3.05$ d or $Z = 0.020$ and $P_{\rm i} = 3.10$ d. We did not try to compute detailed models with lower initial masses, because in such a case, the WD would need to spend a time in excess of the age of the Universe in evolving to the observed configuration. Also, at longer initial periods, models would undergo a common envelope episode because of the very deep outer convective zone of the donor star at the onset of the RLOF.

In our opinion, it is remarkable that the model with $Z = 0.010$ accounts for the masses, the orbital period of the system and the brightness of the WD observed by Lundgren et al. (1996) at the

correct age. We consider it as a successful fit which, in turn, indicates that the stellar evolution processes relevant for the present system are fairly well known. Notice that we would have been able to predict the absolute magnitude of the WD in PSR J1713+0747 system with a reasonable accuracy. Our models fit the main characteristics of the WD at the age corresponding to $\tau_{\rm PSR} = 8$ Gyr given by Splaver et al. (2005). Consequently, we do not find evidence for a faster cooling as in Hansen & Phinney (1998).

However, as our models predict pure hydrogen atmospheres, they are unable to reproduce the colours measured by Lundgren et al. (1996) within the error bars of the observations. In any case, we should remark that this discrepancy is moderate since theory and observations differ by less than 3σ. Moreover, the available photometric data are not yet accurate enough to determine a precise effective temperature and atmospheric chemical composition of the WD companion of the pulsar. In order to get a deeper understanding of the evolution of this system, it would be essential to perform new spectroscopic and photometric observations. Particularly, infrared observations can offer much extra information and may help to constrain this binary further.

ACKNOWLEDGMENTS

OGB has been supported by FONDAP Centre for Astrophysics 1501003. RDR acknowledges partial support from SeCyT-UNC 123/04 and CONICET 691/04.

REFERENCES

Alpar M. A., Cheng A. F., Ruderman M. A., Shaham J., 1982, Nat, 300, 728
Althaus L. G., Serenelli A. M., Benvenuto O. G., 2001, MNRAS, 323, 471
Benvenuto O. G., De Vito M. A., 2003, MNRAS, 342, 50
Benvenuto O. G., De Vito M. A., 2004, MNRAS, 352, 249
Benvenuto O. G., De Vito M. A., 2005, MNRAS, 362, 891
Bergeron P., Saumon D., Wesemael F. 1995, ApJ, 443, 764
Bergeron P., Leggett S. K., Ruiz M. T., 2001, ApJS, 133, 413
Bessell M. S., 1990, PASP, 102, 1181
Borysow A., Jorgensen U. G., Fu Y., 2001, J. Quant. Spectrosc. Radiat. Transfer, 68, 235
Burstein D., Heiles C., 1982, AJ, 87, 1165
Camilo F., Foster R. S., Wolszczan A., 1994, ApJ, 437, L39
Foster R. S., Wolszczan A., Camilo F., 1993, ApJ, 410, L91
Gaur V. P., Tripathi B. M., Joshi G. C., Pande M. C., 1988, ApSS, 147, 107
Gustafsson M., Frommhold L., 2001, ApJ, 546, 1168
Hansen B. M. S., Phinney E. S., 1998, MNRAS, 294, 569
Harris G. J., Lynas-Gray A. E., Miller S., Tennyson J., 2004, ApJ, 617, L143
Jorgensen U. G., Hammer D., Borysow A., Falkesgaard J., 2000, A&A, 361, 283
Kaspi V. M., Taylor J. H., Ryba M. F., 1994, ApJ, 428, 713
Lundgren S. C., Foster R. S., Camilo F., 1996, in ASP Conf. Ser. Vol. 105, IAU Colloq. 160: Pulsars: Problems and Progress. Astron. Soc. Pac., San Francisco, p. 497
McCook G. P., Sion E. M., 1987, ApJS, 65, 603
Monet D. G., Dahn C. C., Vrba F. J., Harris H. C., Pier J. R., Luginbuhl C. B., Ables H. D., 1992, AJ, 103, 638
Nelson L. A., Dubeau E., MacCannell K. A., 2004, ApJ, 616, 1124
Podsiadlowski P., Rappaport S., Pfahl E. D., 2002, ApJ, 565, 1107
Rappaport S., Verbunt F., Joss P. C., 1983, ApJ, 275, 713
Rappaport S., Podsiadlowski P., Joss P. C., Di Stefano R., Han Z., 1995, MNRAS, 273, 731
Rohrmann R. D., 2001, MNRAS, 323, 699
Rohrmann R. D., Serenelli A. M., Althaus L. G., Benvenuto O. G., 2002, MNRAS, 335, 499
Sarna M. J., Ergma E., Gerskevits-Antipova J., 2000, MNRAS, 316, 84
Schönberner D., Driebe T., Blöcker T., 2000, A&A, 356, 929
Serenelli A. M., Althaus L. G., Rohrmann R. D., Benvenuto O. G., 2001, MNRAS, 325, 607
Splaver E. M., Nice D. J., Stairs I. H., Lommen A. N., Backer D. C., 2005, ApJ, 620, 405
Stairs I. H., 2004, Sci, 304, 547
Stancil P. C., 1994, ApJ, 430, 360
Thorsett S. E., Chakrabarty D., 1999, ApJ, 512, 288
van Straten W., Bailes M., Britton M., Kulkarni S. R., Anderson, S. B., Manchester R. N., Sarkissian J., 2001, Nat, 412, 158

This paper has been typeset from a TEX/LATEX file prepared by the author.